Supporting Information

Superelastic Pseudocapacitors from Freestanding MnO$_2$-Decorated Graphene-Coated Carbon Nanotube Aerogels

Yepin Zhao, Maxwell P. Li, Siyuan Liu, and Mohammad F. Islam[*]

Department of Materials Science and Engineering, Carnegie Mellon University, 5000 Forbes Avenue, Pittsburgh, Pennsylvania 15213-3815, United States

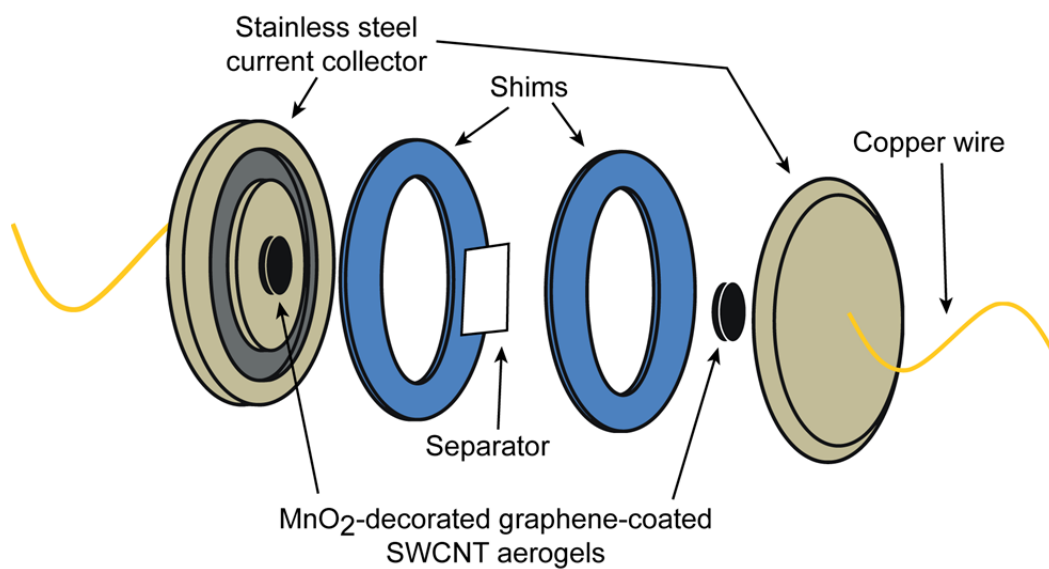E-mail: mohammad@cmu.edu. Phone: (412) 268-8999. Fax: (412) 268-7596

Figure S1. A schematic of a home-built parallel-plate electrochemical testing setup. Compressive strain on the electrodes was adjusted by adding and removing shims from the cell.
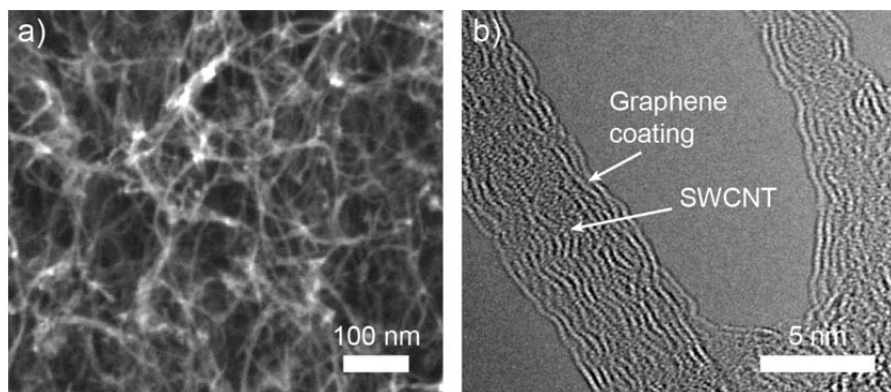
Figure S2. (a) SEM and (b) high-resolution TEM images of a cross-section of graphene-coated SWCNT aerogels show an open porous network with two to five layers of graphene coating on the junctions between SWCNTs and the struts.[1-5]
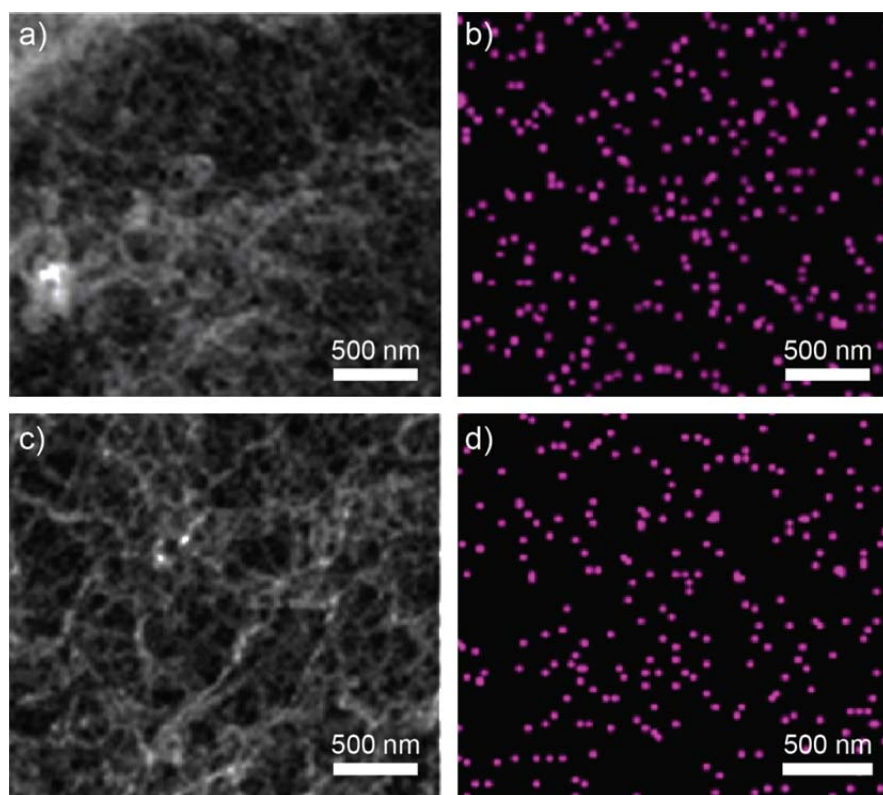
Figure S3. SEM images (a, c) and corresponding EDS mapping of Mn (b, d) at the surfaces (a, b) and the interior (c, d) of MnO_2-decorated graphene-coated SWCNT aerogels after 10 000 charge–discharge cycles.
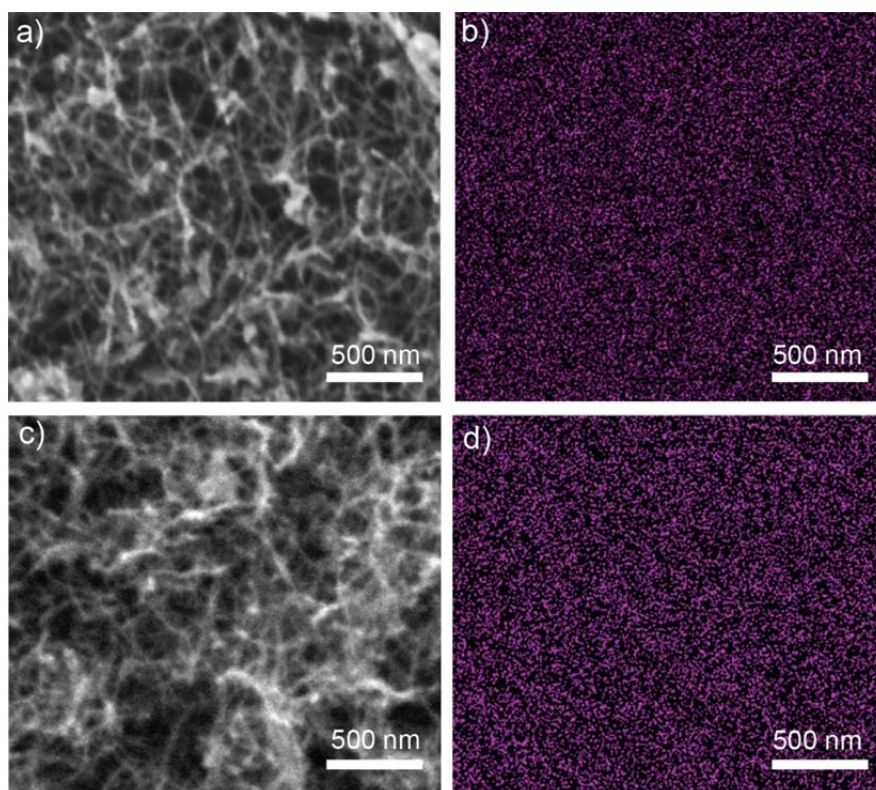
Figure S4. SEM images (a, c) and corresponding EDS mapping of Mn (b, d) at the surfaces (a, b) and the interior (c, d) of MnO$_2$-decorated graphene-coated SWCNT aerogels after 10 000 compression–release cycles but before any charge–discharge cycles.
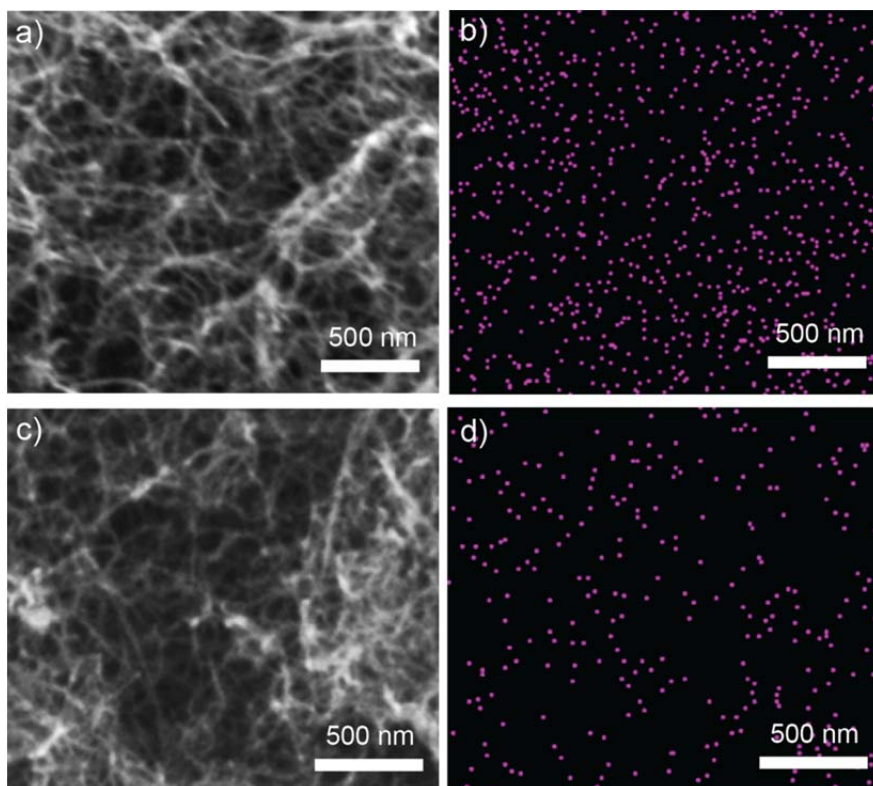
Figure S5. SEM images (a, c) and corresponding EDS mapping of Mn (b, d) at the surfaces (a, b) and the interior (c, d) of MnO$_2$-decorated graphene-coated SWCNT aerogels after 10 000 compression–release and subsequent 10 000 charge–discharge cycles.
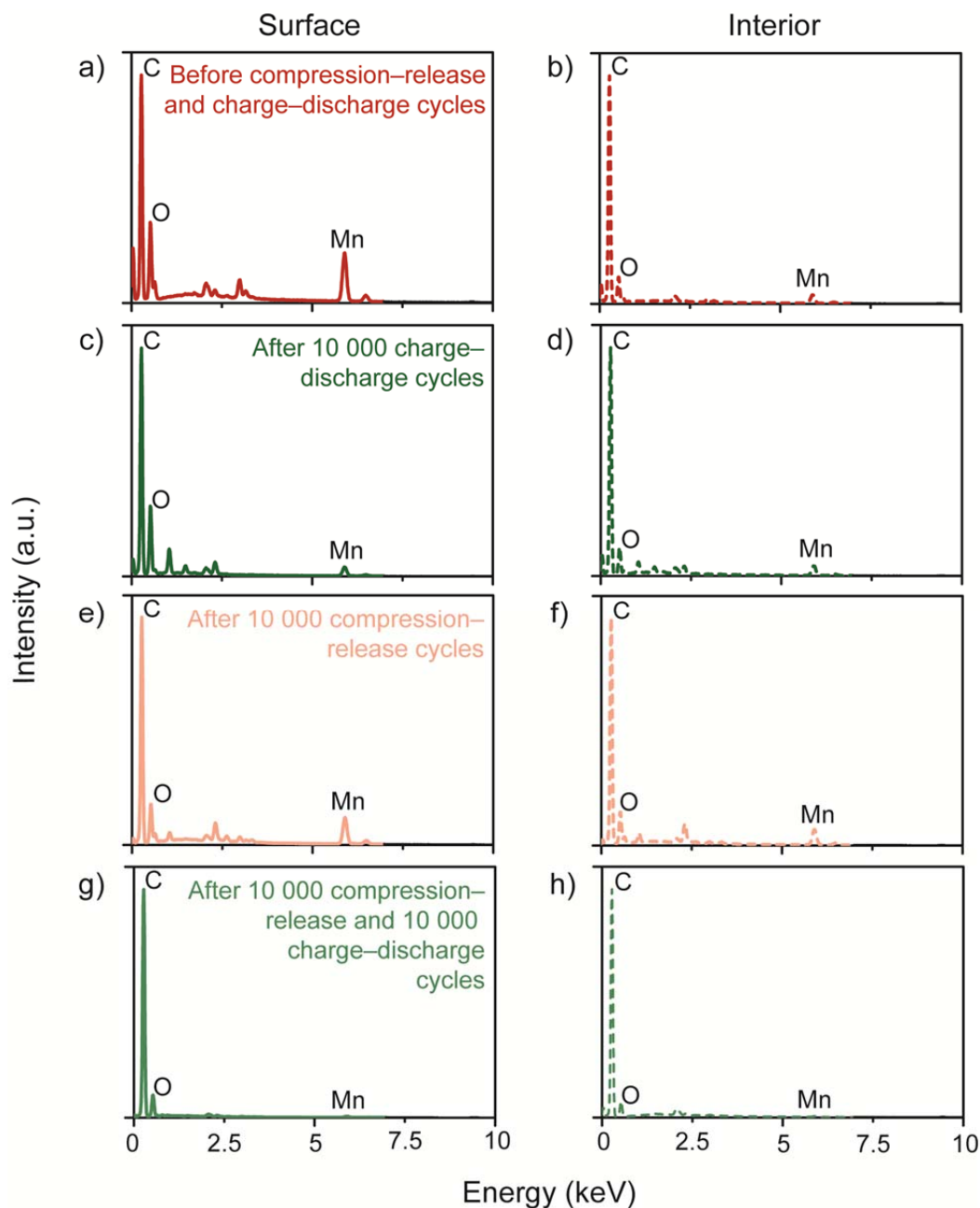
Figure S6. EDS spectra from MnO_2-decorated graphene-coated SWCNT aerogels (a, b) before any compression–release and charge–discharge cycles, (c, d) after 10 000 charge–discharge cycles, (e, f) after 10 000 compression–release cycles, and (g, h) after 10 000 compression– release and subsequent 10 000 charge–discharge cycles. Samples were examined at the surfaces (a, c, e, and g) and the interior (b, d, f, and h). MnO_2 weight percentages were from weight percentages of carbon and manganese detected in EDS spectra and also accounting for the oxygen in MnO_2.
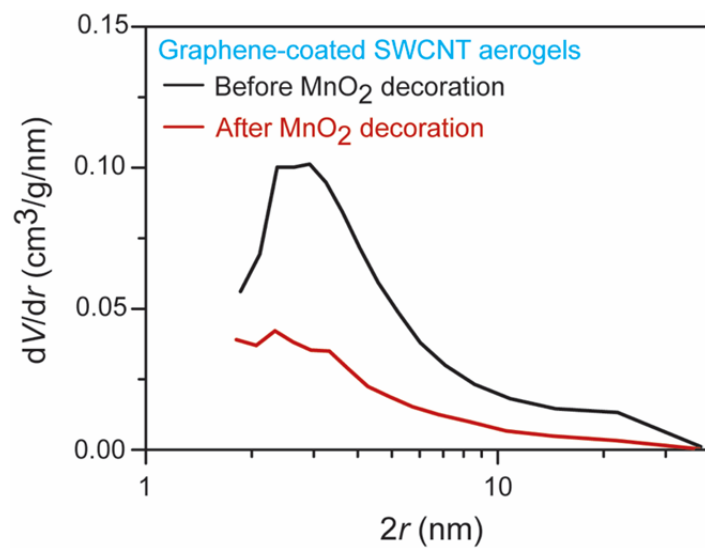
Figure S7. The pore diameter distribution of graphene-coated SWCNT aerogels before and after MnO_2 decoration using the desorption branch of the isotherm and the BJH analysis. A majority of the pores is between 2–40 nm in diameter for both types of aerogels.
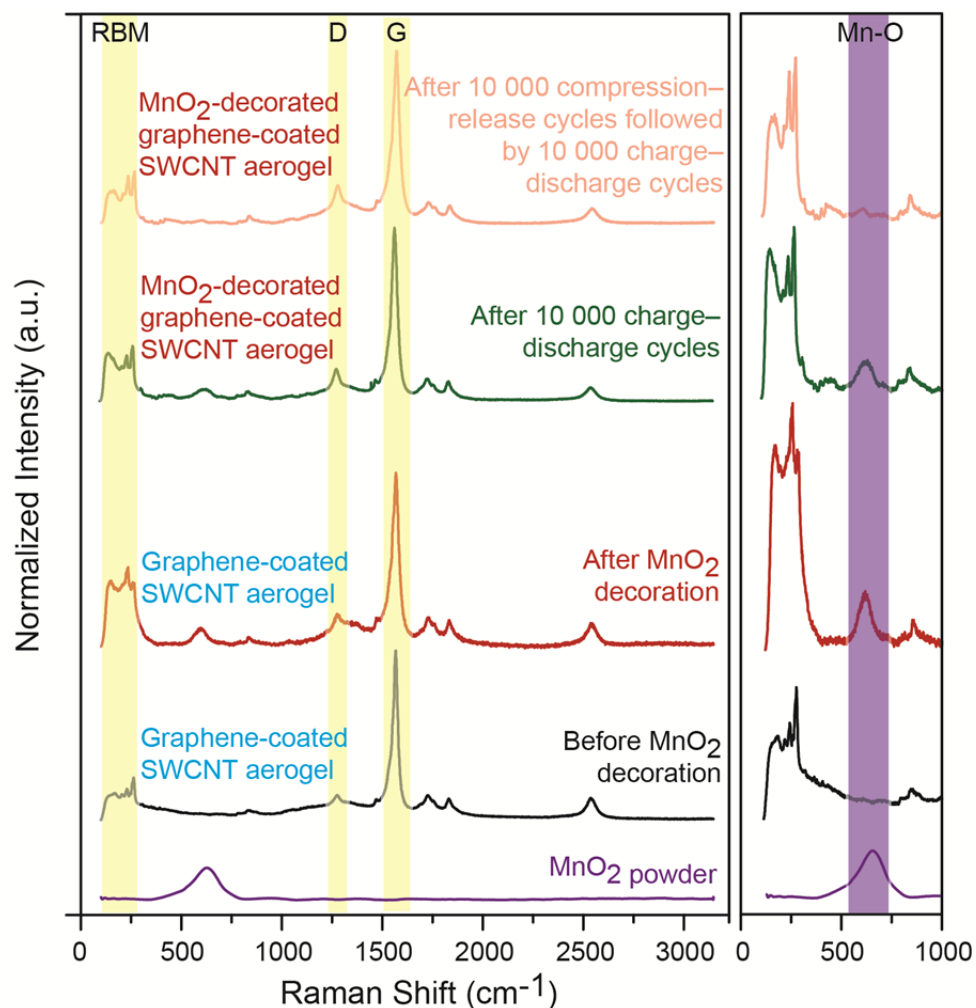
Figure S8. Raman spectra from graphene-coated SWCNT aerogels before and after MnO₂ decoration as well as MnO₂-decorated graphene-coated SWCNT aerogels after 10 000 charge–discharge cycles and after 10 000 compression–release cycles followed by 10 000 charge–discharge cycles. Each spectrum is normalized by the intensity of the G-band of the SWCNTs at ~1590 cm^{-1}.
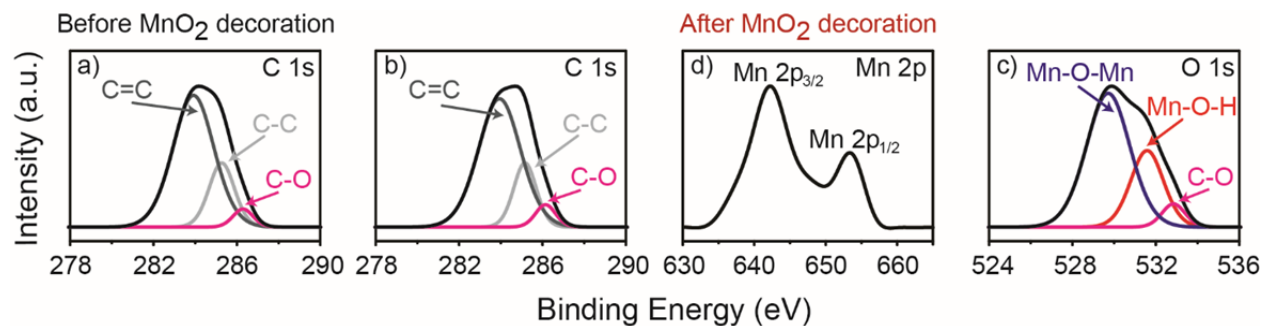
Figure S9. XPS spectra from graphene-coated SWCNT aerogels (a) before and (b, d) after MnO_2 decoration. C 1s spectra (a) before and (b) after MnO_2 deposition. (c) Mn 2p and (d) O 1s spectra after MnO_2 deposition.

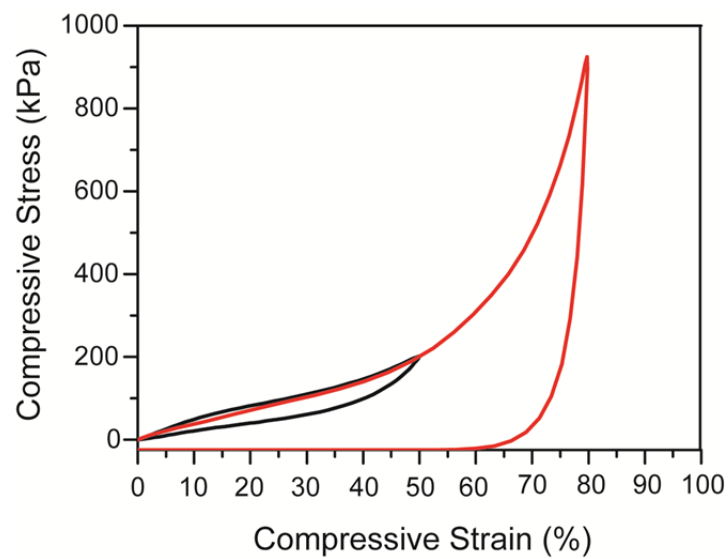**Figure S10.** Compressive stress vs compressive strain curves of MnO_2-decorated graphene-coated SWCNT aerogels. The aerogels display 48% plastic deformation when compressed to 80% strain, whereas compression to 50% strain does not induce any plastic deformation.
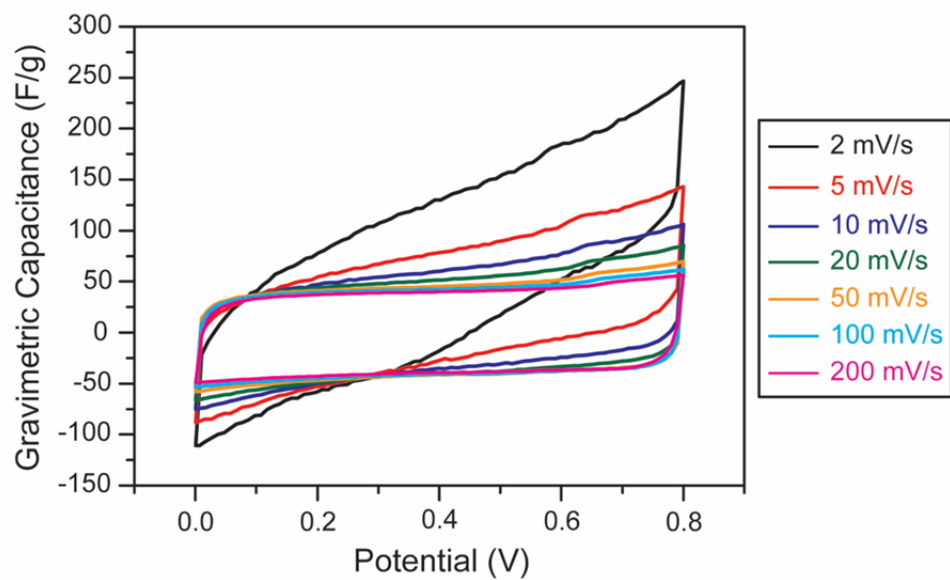
Figure S11. Cyclic voltammograms of MnO$_2$-decorated graphene-coated SWCNT aerogels before compression at scan rates from 2–200 mV/s.

Figure S12. Electrochemical performance of MnO$_2$-decorated graphene-coated SWCNT aerogels before compression and after 10 000 compression–release cycles. (a) Representative galvanostatic charge–discharge curves at 1 A/g and (b) Nyquist plots depict near identical performance even after being subjected to vigorous mechanical deformation.
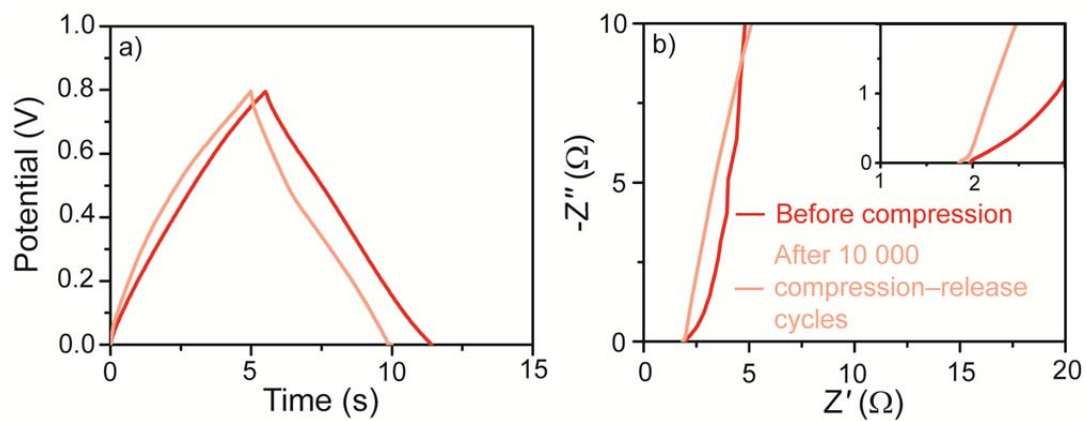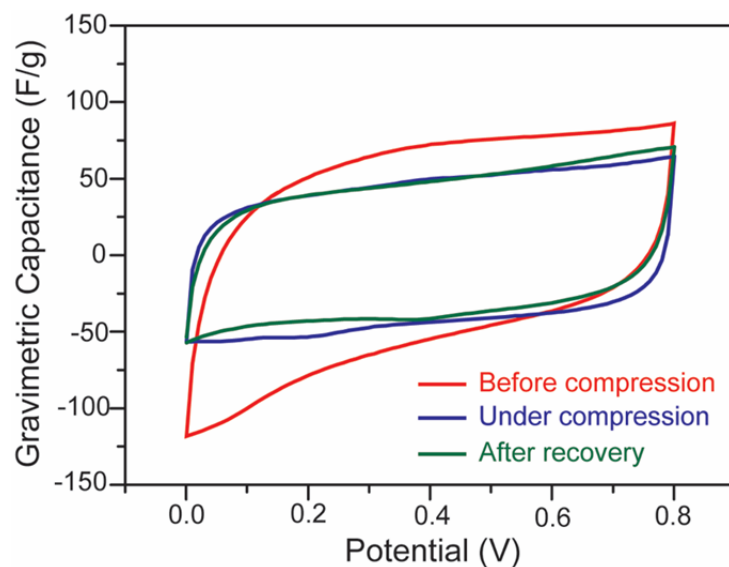
Figure S13. Cyclic voltammograms of MnO_2-decorated graphene-coated SWCNT aerogels with greater MnO_2 loading (33 wt%) before, under, and after recovery from 50% compression at a scan rate of 100 mV/s. The electrodes exhibit nearly identical gravimetric capacitances under compression and after recovery from compression to 50% strain. However, gravimetric capacitance of the aerogels is slightly larger before compression.

Figure S14. Gravimetric capacitances of MnO$_2$-decorated graphene-coated SWCNT aerogels with 33 wt% MnO$_2$ loading before and under 50% compression over a scan rate of 2–200 mV/s.

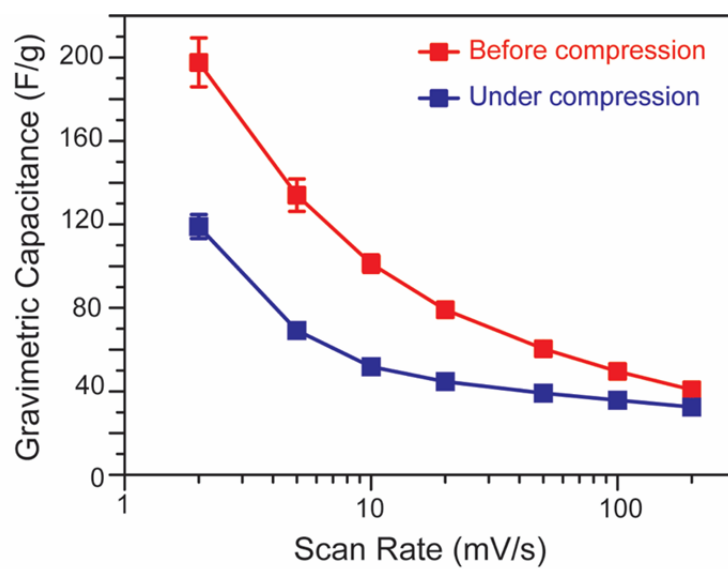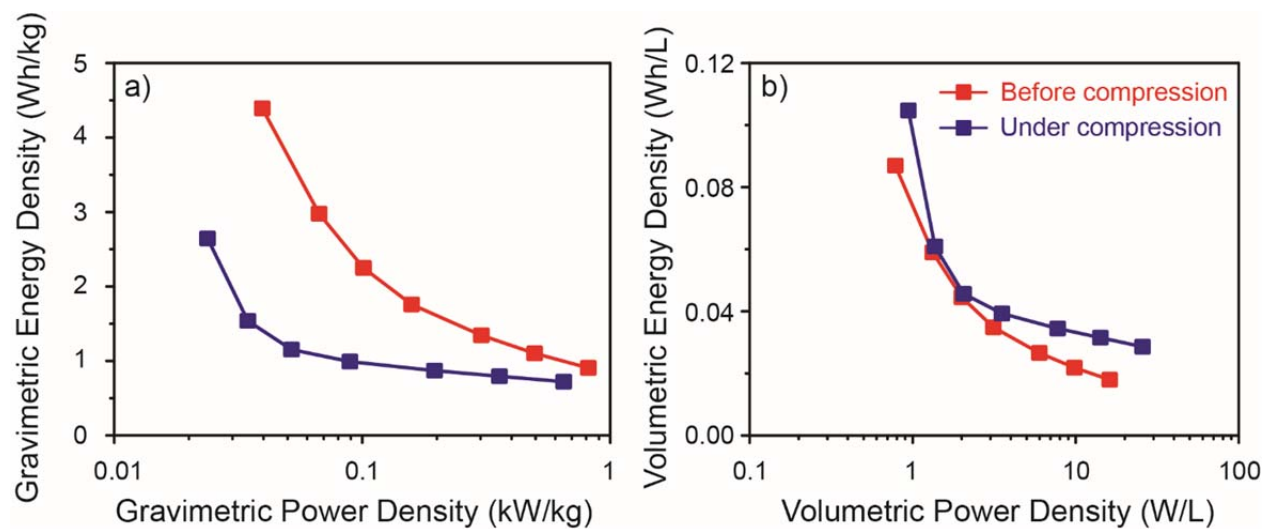**Figure S15.** (a) Gravimetric and (b) volumetric energy versus power densities for MnO_2-decorated graphene-coated SWCNT aerogels with 33 wt% MnO_2 loading before and under 50% compression.

Table S1. Comparison of compressible pseudocapacitors

pseudocapacitive material	capacitance before compression	maximum compressive strain (%)	capacitance under maximum compression	capacitance after recovery from maximum compression	number of compression−release cycles; strain (%)	reference
MnO_2	98 F/g 1.5 F/cm^3	50	106 F/g 3.3 F/cm^3	128 F/g 2.0 F/cm^3	10 000; 50	this work
Polypyrrole and MnO_2	320 F/g 9 F/cm^3	50	293 F/g 16 F/cm^3	N/A	N/A	ref 6
Polypyrrole	310 F/g 9.8 F/cm^3	50	288 F/g 18.2 F/cm^3	304 F/g 9.6 F/cm^3	1 000; 50	ref 7
Polypyrrole	360 F/g 14 F/cm^3	50	350 F/g 27.2 F/cm^3	360 F/g 14 F/cm^3	1 000; 50	ref 8
Polyaniline	216 F/g 3.4 F/cm^3	60	209 F/g 8.2 F/cm^3	209 F/g 3.3 F/cm^3	100; 60	ref 9
MnO_2	212 F/g 2.2 F/cm^3	80	105.4 F/g 6.4 F/cm^3	N/A	N/A	ref 10
Polypyrrole	753.8 F/g 1.4 F/cm^3	80	592.3 F/g 5.5 F/cm^3	N/A	N/A	ref 10
α-Fe_2O_3	296.3 F/g 2.8 F/cm^3	70	266.7 F/g 8.3 F/cm^3	296.3 F/g 2.8 F/cm^3	1 000; 50	ref 11

References

(1) Kim, K. H.; Oh, Y.; Islam, M. F., Graphene Coating Makes Carbon Nanotube Aerogels Superelastic and Resistant to Fatigue. *Nat. Nanotechnol.* **2012,** *7* (9), 562–566.

(2) Wilson, E.; Islam, M. F., Ultracompressible, High-Rate Supercapacitors from Graphene-Coated Carbon Nanotube Aerogels. *ACS Appl. Mater. Interfaces* **2015,** *7* (9), 5612–5618.

(3) Campbell, A. S.; Jose, M. V.; Marx, S.; Cornelius, S.; Koepsel, R. R.; Islam, M. F.; Russell, A. J., Improved Power Density of an Enzymatic Biofuel Cell with Fibrous Supports of High Curvature. *RSC Adv.* **2016,** *6* (12), 10150–10158.

(4) Tsui, M. N.; Islam, M. F., Creep- and Fatigue-Resistant, Rapid Piezoresistive Responses of Elastomeric Graphene-Coated Carbon Nanotube Aerogels over a Wide Pressure Range. *Nanoscale* **2017,** *9* (3), 1128–1135.

(5) Kim, K. H.; Tsui, M. N.; Islam, M. F., Graphene-Coated Carbon Nanotube Aerogels Remain Superelastic while Resisting Fatigue and Creep over −100 to +500 °C. *Chem. Mater.* **2017,** *29* (7), 2748–2755.

(6) Li, P.; Yang, Y.; Shi, E.; Shen, Q.; Shang, Y.; Wu, S.; Wei, J.; Wang, K.; Zhu, H.; Yuan, Q.; Cao, A.; Wu, D., Core-Double-Shell, Carbon Nanotube@Polypyrrole@MnO_2 Sponge as Freestanding, Compressible Supercapacitor Electrode. *ACS Appl. Mater. Interfaces* **2014,** *6* (7), 5228–5234.

(7) Li, P.; Shi, E.; Yang, Y.; Shang, Y.; Peng, Q.; Wu, S.; Wei, J.; Wang, K.; Zhu, H.; Yuan, Q.; Cao, A.; Wu, D., Carbon Nanotube-Polypyrrole Core-Shell Sponge and its Application as Highly Compressible Supercapacitor Electrode. *Nano Res.* **2014,** *7* (2), 209–218.

(8) Zhao, Y.; Liu, J.; Hu, Y.; Cheng, H.; Hu, C.; Jiang, C.; Jiang, L.; Cao, A.; Qu, L., Highly Compression-Tolerant Supercapacitor Based on Polypyrrole-Mediated Graphene Foam Electrodes. *Adv. Mater.* **2013,** *25* (4), 591–595.

(9) Niu, Z.; Zhou, W.; Chen, X.; Chen, J.; Xie, S., Highly Compressible and All-Solid-State Supercapacitors Based on Nanostructured Composite Sponge. *Adv. Mater.* **2015,** *27* (39), 6002–6008.

(10) Xu, C.; Li, Z.; Yang, C.; Zou, P.; Xie, B.; Lin, Z.; Zhang, Z.; Li, B.; Kang, F.; Wong, C. P., An Ultralong, Highly Oriented Nickel-Nanowire-Array Electrode Scaffold for High-Performance Compressible Pseudocapacitors. *Adv. Mater.* **2016,** *28* (28), 5777–5777.

(11) Cheng, X.; Gui, X.; Lin, Z.; Zheng, Y.; Liu, M.; Zhan, R.; Zhu, Y.; Tang, Z., Three-Dimensional α-Fe_2O_3/Carbon Nanotube Sponges as Flexible Supercapacitor Electrodes. *J. Mater. Chem. A* **2015,** *3* (42), 20927–20934.